EurJIC
European Journal of Inorganic Chemistry

Chemistry Europe
European Chemical Societies Publishing

Accepted Article

Title: Tuning the gold(I)-carbon σ bond in gold-alkynyl complexes through structural modifications of the NHC ancillary ligand: effect on spectroscopic observables and reactivity

Authors: Diego Sorbelli, Paola Belanzoni, and Leonardo Belpassi

To be cited as: *Eur. J. Inorg. Chem.* 10.1002/ejic.202100260

Link to VoR: https://doi.org/10.1002/ejic.202100260

WILEY-VCH

10.1002/ejic.202100260

Tuning the gold(I)-carbon σ bond in gold-alkynyl complexes through structural modifications of the NHC ancillary ligand: effect on spectroscopic observables and reactivity

Diego Sorbelli,*[a] Paola Belanzoni*[a,b] and Leonardo Belpassi*[b]

[a] D. Sorbelli, Prof. Dr. P. Belanzoni
Department of Chemistry, Biology and Biotechnology
University of Perugia
Via Elce di Sotto 8, I-06123, Perugia, Italy
E-mail: *diegosorbelli00@gmail.com* ; *paola.belanzoni@unipg.it*
[b] Dr. Leonardo Belpassi, Prof. Dr. P. Belanzoni
CNR Institute of Chemical Science and Technologies “Giulio Natta” (CNR-SCITEC), c/o Department of Chemistry, Biology and Biotechnology, University of Perugia
Via Elce di Sotto 8, I-06123, Perugia, Italy
E-mail: *leonardo.belpassi@cnr.it*

Abstract

Understanding the features of the gold(I)-carbon σ bond and its modulation induced by an ancillary ligand has become fundamental for the purposes of ligand design, due to the increasing interest towards gold(I)-alkynyl complexes and their wide range of applications. We carry out a systematic computational analysis of 16 gold(I)-acetylide complexes bearing different N-Heterocyclic Carbenes (NHCs) as ancillary ligands [NHCs-Au(I)-CCH]. The results show that the strength and features of the Au-C bond can be efficiently tuned by performing specific structural modifications on the NHC, enabling a more efficient π communication between the alkynyl and the ancillary ligand. We also demonstrate that the effect of the bond modulation can be revealed via NMR spectroscopy, as highlighted by the tight correlation between the computed nuclear shielding constants and the bonding parameters. Finally, we show that, for the dual-gold-catalyzed Bergman cyclization as case study, suitable structural modifications on the NHC ligand, which modulate the π-acidity of the metal fragment σ-coordinated to an enediyne substrate, could affect the reaction barrier and the thermodynamic stability of the product. All the reported results can be well rationalized in the framework of distortion/interaction analysis, which has been recently extended to the dual (σ,π-type) Au catalytic systems by Alabugin et al. (J. Am. Chem. Soc. 2017, 139, 3406-3416).

Introduction

Gold(I)-alkynyl (LAu(I)CCR) complexes represent a class of versatile gold compounds which have proven to be potentially very useful for several practical applications.[1]

For instance, the biological activity of Au(I)-alkynyl complexes has received an increasing interest in the last years, in particular related to their anticancer activity and their potential applications in bioimaging and therapy. These compounds show a remarkable stability in vitro and diverse biological properties can be induced by different ancillary ligands (L).[2–4] These gold complexes also display very interesting optical properties, due to both the heavy atom effect, which is able to induce phosphorescence emission, and the versatile attitude of the alkynyl moiety (behaving as π-donor, π-acceptor and σ-donor), that can tune the emission behavior in both isolated complexes[5] and molecular rods.[6]

Recently, gold-alkynyl complexes have become attractive also in the framework of gold catalysis[7–10] with the discovery of the dual-activation mode (dual σ,π-catalysis)[11,12]. In dual catalysis one gold fragment η^2-coordinates to an alkyne moiety (π mode), whereas the other gold center is bound to the alkynyl fragment via a η^1 coordination (σ mode).[13] Since then, this new catalytic route has received an ongoing amount of attention, since it allows to efficiently access cyclizations, C,H-activations (even combined with halogen transfer reactions) and new synthetic routes for carbo- and heterocycles.[11] It has been recently reported that the dual-catalytic mode is particularly favorable in the framework of gold-catalyzed Bergman cyclization (BC).[14]

By photoelectron spectroscopy, Liu and coworkers were able to experimentally characterize a series of gold-acetilyde complexes ($[LAuCCH]^-$, L=Cl^- ,I^- ,CCH^-) and, assisted by quantum chemical calculations, they were able to demonstrate that the gold-carbon σ bond is among the strongest gold-substrate bonds, by far stronger than the well-known gold-alkyne π bond and comparable to the strong gold-cyano bond in gold dicyanoaurate.[15] They also showed that, surprisingly, the Au-C bond is extremely sensible to the ancillary ligand, with higher electronegative ligands determining a stronger gold-carbon interaction. Further studies on this series of gold-acetylide complexes by quantum chemical calculations revealed that the Au-C bond in these complexes can be described within a resonance-type three-center-four-electron picture, with the ancillary ligand L playing a determining role in modulating the strength of this bond via hyperconjugative interactions.[16] Thus, it is clear that the nature and the electronic

structure of the ancillary ligand L are a viable and efficient way of modulating the gold-alkynyl interaction.

N-Heterocyclic Carbenes (NHCs) represent a class of ligands that are very popular in transition metals catalysis[17–19] and widely used for Au(I) complexes due to the stability of the metal-carbene bond they form[20] and the efficient catalytic properties of NHC-metal compounds.[21]

The first isolable NHC has been synthesized 30 years ago by Arduengo et al.[22] and, during the years, these species have been discovered to possess a wide range of electronic properties that are quite intriguing. Indeed, they can behave as σ-donors using the lone pair located on C(sp^2), but also as π-acceptors, involving the formally empty p orbital perpendicular to the NHC plane.

Remarkably, the electronic properties of NHCs can be tuned via structural modifications. Upon the discovery of new classes of carbenes, such as cyclic(alkyl)(amino)carbenes (CAACs)[23] and diamidocarbenes (DACs)[24–26] , the electronic properties of carbene ligands could be extensively modulated, in particular concerning their π-donor and π-acceptor properties. Recently Frenking et al. presented theoretical evidence of the relationship between the structures of the carbenes and their π-acceptor properties, with CAACs and DACs possessing an enhanced π-acid behavior due to a reduced internal π-donation to the carbenic carbon atom.[27] Other studies support these results by highlighting how their electronic properties vary sensibly upon changes in their structure[28,29] which have also been probed experimentally by ^{77}Se[30,31] and ^{31}P[32] NMR spectroscopy. Concerning the interaction of NHCs with transition metals, and specifically gold, it has been demonstrated that such π interactions are fundamental for the formation of the well-known strong carbene-metal bond[33,34]. In this framework, it has been shown by some of us that the π-accepting ability of NHCs in gold(I)-NHC adducts can be easily tuned by applying selected structural modifications on the NHC backbone, such as the ring size, the nature of the heteroatoms, the aromaticity of the backbone and the nature of the alkyl and aryl groups on the nitrogen atoms which are of importance since, due to their σ-withdrawing and π-donating effect, they stabilize the carbenic carbon.[20,35,36] In particular, the π-accepting ability of NHC can be modulated even inducing a modification of the π back-donation ability of the gold metal fragment.[37]

All the factors discussed above motivated us to study the modulation of the Au-C bond in a series of 16 neutral gold-acetylide complexes (NHC-Au(I)-CCH), where the backbone, the aromaticity and the substituents on the nitrogen atoms of the NHC ancillary ligand are

modified. We performed such structural modifications with the aim of modulating the Au-CCH bond. We chose the different NHC ligands on the basis of the results reported in the systematic analysis carried out in Ref. [37]. The NHC-Au(I)-CCH complexes under study in this work are depicted in Scheme 1. Starting from complex **1** as prototype, we replaced the hydrogen atoms on the N atoms of the NHC with alkyl (**2a**, **2c**, **2d**) and aryl (**2b**, **2e**, **2f**) groups. Then, we introduced oxygen atoms in the backbone of the carbene (**3a**-**3d**): remarkably, similar NHCs have shown unique catalytic activity in some gold catalyzed reactions.[38] In **3c** and **3d** the size of the ring is also increased from five to six members. We also modified the backbone of the NHC by changing its unsaturation (**4** and **5**). Finally, we modified the NHC by changing the heteroatom on the ring, i.e. by removing a nitrogen atom, thus obtaining pyrrolidenes (**6a**-**6b**) and thiazolidenes (**7**). We note that the NHCs studied here represent commonly used ligands in gold catalysis.

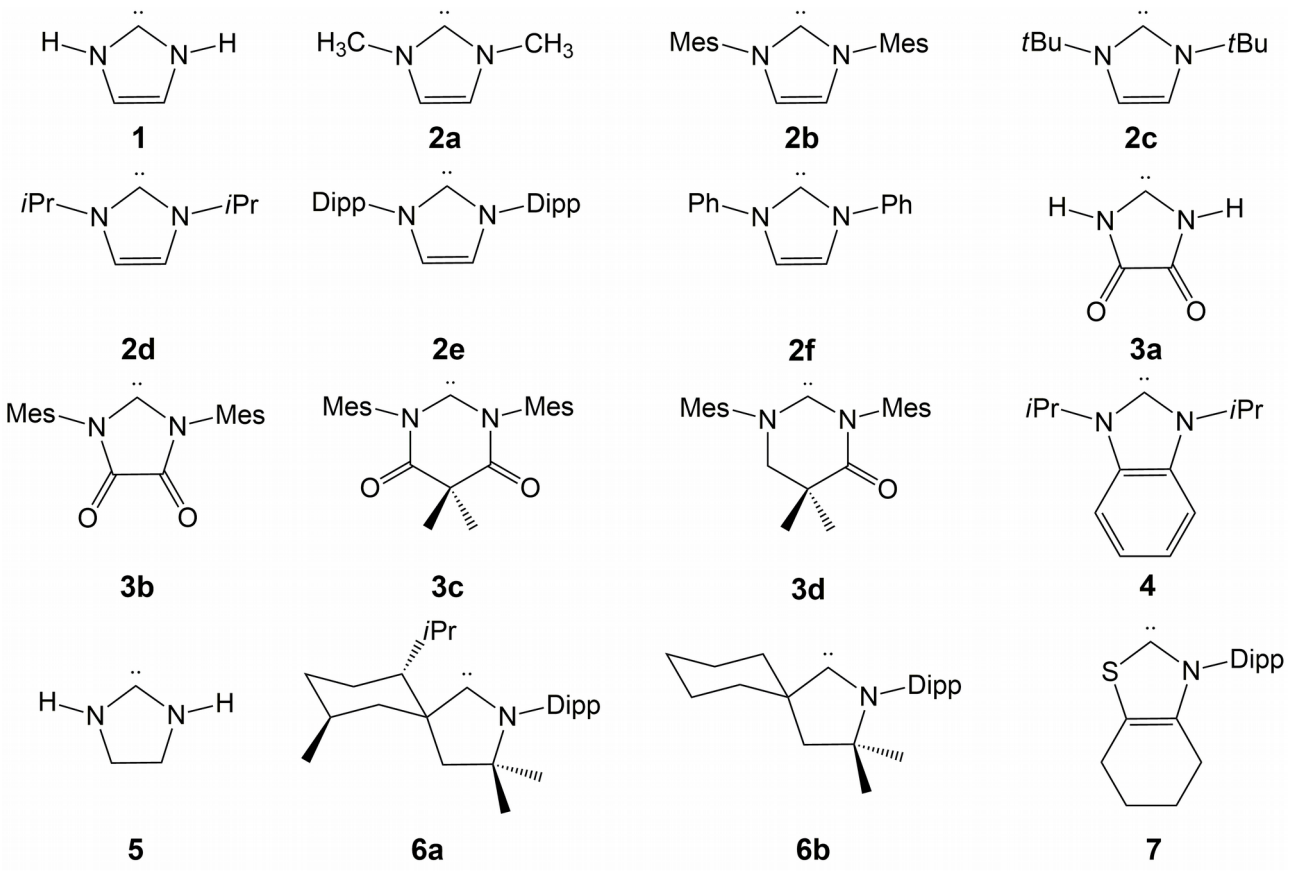

Scheme 1. Structures of the 16 different NHC ligands used for the gold-alkynyl bond analysis in NHC-Au(I)-CCH complexes. (*iPr*=isopropyl, *tBu*=*tert*-butyl, *Mes*=1,3,5-trimethylbenzene, *Dipp*=2,6-diisopropylphenyl).

In this work, a systematic and in-depth computational analysis of the gold-carbon bond is carried out for this series of NHC-Au(I)-CCH complexes. In particular the Charge-Displacement analysis has been applied in combination with the Natural Orbitals for Chemical Valence scheme (CD-NOCV)[39] to obtain a detailed picture of the bond, in order to highlight the bonding features that can be influenced by the structural modifications of the NHC (see Scheme 1). In addition, we also explored how in these complexes the tunable bonding features (extent of alkynyl-to-metal fragment σ donation and π communication between the alkynyl and the metal fragment) can be revealed experimentally by calculating their spectroscopic properties (in particular by ^{13}C NMR of alkynyl carbons) and to which extent they are affected by the structural modifications. We have also included in our analysis a NHC-gold(I)-phenylethynyl complex (**2a**-Au(I)-**Ph**), which has been recently characterized and which shows an interesting biological activity,[40] and the **3b**-Au(I)-**Ph** complex, in order to demonstrate how the overall results may have a general relevance for gold-alkynyl complexes (see Scheme 2).

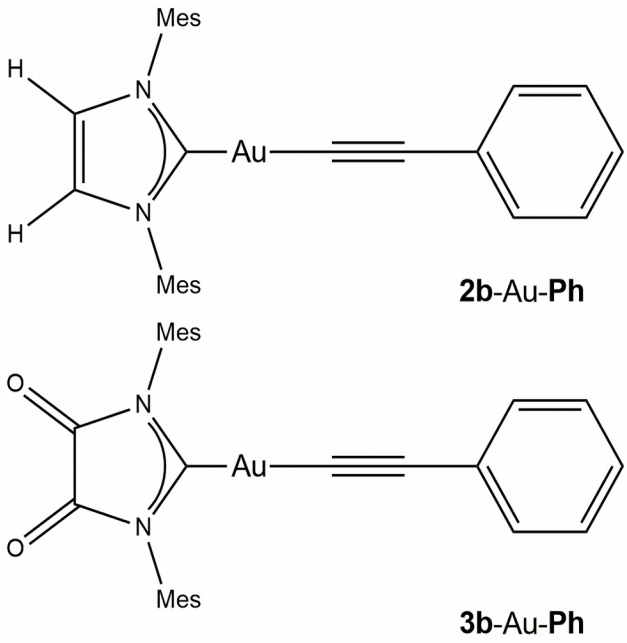

Scheme 2. Structures of the phenylethynyl gold-NHC complexes (**2b**-Au-**Ph** and **3b**-Au-**Ph**)

Finally, we investigated the structure/reactivity relationship by modelling the σ,π dual gold catalysis of Bergman cyclization (BC) using different NHCs according to their electronic properties and we found a clear relationship between the π withdrawing ability of NHC and the catalytic efficiency in the case of the BC. This evidence has been rationalized within the

10.1002/ejic.202100260

distortion/interaction analysis, that was recently extended to the framework of cyclization reactions.[14]

Methodology

For the analysis of the Au-alkynyl bond in the NHC-Au-CCH complexes **1**-**7** (Scheme 1) and in **2b**-Au-**Ph** and **3b**-Au-**Ph** complexes (Scheme 2), the Charge Displacement (CD) analysis via Natural Orbitals for Chemical Valence (NOCV) scheme has been used.[39] The CD-NOCV analysis is a useful tool for analyzing the coordination bond, since it allows to quantify the amount of electronic charge that is transferred between two fragments (A and B) upon the formation of the A-B bond. The Charge Displacement function (Δq) is defined as the partial progressive integration on a suitable z-axis of the electron density difference ($\Delta\rho$) between the density of the adduct (A-B) and the sum of the densities of the non-interacting fragments (A and B) at the positions they have in the adduct geometry:[41]

$$\Delta q(z) = \int_{-\infty}^{z} dz' \int_{-\infty}^{+\infty}\int_{-\infty}^{+\infty} \Delta\rho(x,y,z')\,dxdy \qquad [1]$$

In equation [1], the integration axis is conveniently chosen as the bond axis between the two fragments constituting the adduct. In this work, the fragments are the metal fragment ([NHC-Au]$^{+}$) and the alkynyl ligand ([CCH]$^{-}$) and the z-axis coincides with the bond axis joining the Au nuclei and the σ coordinated carbon (C1) of the alkynyl moiety.

The CD function, $\Delta q(z)$, quantifies at each point of the bond axis the exact amount of electron charge that, upon formation of the bond, is transferred from the right to the left across a plane perpendicular to the bond axis through z. We choose to evaluate, as usual, the charge transfer (*CT*) between A and B, by taking the CD value at the "isodensity boundary", i.e. the z-point where equally valued isodensity surfaces of the isolated fragments become tangent.[41,42] The CD analysis has been previously used to characterize interactions between noble gases and Au, adducts with hydrogen- or halogen-bonds,[43–45] gold complexes[41,46–48]and electronic excited states.[49] The CD-NOCV scheme is very useful when describing the coordination bond in transition metal complexes because it is able to give a quantitative picture of the bond in terms of its Dewar-Chatt-Duncanson (DCD) components (i.e. σ donation and π back-donation) even in those cases in which the metal complexes do not possess specific molecular symmetry. More in detail, in the NOCV scheme,[50,51] the occupied orbitals of the two fragments are orthogonalized to each other and renormalized (yielding the so-called "promolecule") and the charge rearrangement taking place upon bond formation is calculated

from the promolecule as reference. The resulting electron density rearrangement can be expressed in terms of NOCV pairs which are defined as the eigenfunctions of the so-called ‘‘valence operator’’[52–54] from Nalewajski and Mrozek valence theory as follows:

$$\Delta\rho' = \sum_k v_k\left(|\phi_{+k}|^2 - |\phi_{-k}|^2\right) = \sum_k \Delta\rho'_k \qquad [2]$$

where ϕ_{+k} and ϕ_{-k} are the NOCV pairs orbitals and $v_{\pm k}$ are the eigenvalues. v_k represents the fraction v_k of electrons that is transferred from the ϕ_{+k} to the ϕ_{-k} orbital upon formation of the adduct. In the CD-NOCV scheme, the density rearrangement due to the bond formation between two fragments ($\Delta\rho'$) can be partitioned in different NOCV deformation densities ($\Delta\rho'_k$) and therefore one is able to quantify the CT associated to each different component. It must be noted that only few of the NOCV pairs contributes to the chemical bond. Therefore, when the CD-NOCV analysis is carried out, usually only the first $\Delta\rho_k$’ components are investigated in order to understand which significant chemical contribution to the bond they represent.

The CD-NOCV scheme has been applied with success in very different contexts to characterize the chemical interactions throughout the whole periodic table, from weak chemical bond involving helium[55] to the coordination bond in gold complexes.[56–58] The method has been found to be particularly useful to single out specific correlations between coordination bonding features and experimental observables.[56,58–62] Using its 4-component relativistic formulation,[63] the coordination and halogen bonds involving heavy elements was studied.[64–66]

In this work we also used the Energy Decomposition Analysis (EDA)[67] to get further and complementary insights into the gold-alkynyl bond. With this approach, the interaction energy between the $[NHCAu]^+$ and $[CCH]^-$ fragments can be decomposed in different contributions as follows:

$$\Delta E_{\text{int}} = \Delta E^{Pauli} + \Delta V_{elst} + \Delta E_{oi} + \Delta E_{disp} \qquad [3]$$

where ΔE^{Pauli} represents the Pauli repulsion interaction between occupied orbitals of the two fragments, ΔV_{elst} represents quasiclassical electrostatic interaction between the unperturbed charge distributions of the fragments at their final positions, ΔE_{disp} represents the dispersion contribution and ΔE_{oi} is the orbital interaction, which arises from the orbital relaxation and the

orbital mixing between the fragments, and accounts for electron pair bonding, charge transfer, and polarization.

The term ΔE_{oi} can be further decomposed within the EDA-NOCV[68] scheme into NOCV pairwise orbital contributions ($\Delta E_{oi} = \sum_k \Delta E_{oi}^k$) which associates an energy contribution (E_{oi}^k) to the NOCV deformation density ($\Delta\rho_k$).

Computational details

Geometry optimizations and harmonic frequencies calculations of gold-alkynyl complexes with different NHCs **1**-**7** (Scheme 1) and of complexes **2b**-Au-**Ph** and **3b**-Au-**Ph** (Scheme 2) have been carried out at the DFT level with the ADF program (version 2014.05),[69,70] using a Slater-type TZ2P basis set, the BP86[71,72] exchange-correlation functional, the approximate 2-component scalar relativistic Hamiltonian ZORA[73–75] for the inclusion of relativistic effects and Grimme's D3 dispersion correction[76] with the Becke-Johnson (BJ) damping scheme.[77] The CD-NOCV analysis and the EDA have been performed with the same computational setup. The NOCV deformation densities have been mapped on a grid (CUBE format) using tools available in the ADF suite (*densf* or directly from ADF-GUI). The CD-NOCV curves have been evaluated numerically using the PYCUBESCD suite of programs.[78] In order to test the effect of the functional, the CD-NOCV analysis has been carried out for the **1**-Au-CCH complex also using the hybrid B3LYP[79] functional. The results (reported in Table S1 and Figure S1 in the Supporting Information) validate the protocol chosen for the analysis, since they are qualitatively and quantitatively comparable.

NMR nuclear shielding constants calculations have been carried out with the ADF code, but with a different computational protocol which has been proven to be very accurate for the calculation of ^{1}H and ^{13}C chemical shifts in gold complexes.[80,81] The hybrid PBE0[82,83] functional was used together with a TZ2P basis set. In this case both scalar relativistic effects and spin-orbit coupling have been introduced by employing the approximate 2-component spin-orbit ZORA Hamiltonian. Gauge-including atomic orbitals (GIAOs)[84] were used and the terms from the exchange-correlation (XC) response kernel were included.[85]

The geometries and frequencies of stationary points (minima with zero imaginary frequencies and transition states with one imaginary frequency) for the gold-catalyzed Bergman cyclization have been calculated using ADF in combination with the related Quantum-regions Interconnected by Local Description (QUILD) program,[86] employing the BP86 functional, the TZ2P basis set with a small frozen core approximation for all atoms, the ZORA Hamiltonian for including scalar relativistic effects and Grimme's D3-BJ dispersion correction. This setup has been proven to yield very accurate structures for model gold-catalyzed processes.[87] This protocol has also been used for the calculation of the Voronoi Deformation Density (VDD) charges.[88] The effect of solvation (toluene) has also been tested by the Conductor-like Screening Model (COSMO) for solvation as implemented in the QUILD program.[89]

Single-point energy calculations for all the stationary points (minima and transition states) have been carried out at the *ab-initio* level with the Domain-based Local Pair Natural Orbital Coupled Cluster method (DLPNO-CCSD(T))[90,91] as implemented in the ORCA software.[92] DLPNO-CCSD(T) has been shown to yield very accurate results (comparable to the regular Coupled-Cluster approach[93]) by keeping the computational cost relatively low (it has been estimated that its computational cost is only two to four times the cost of DFT[94]). The calculations have been carried out by using Ahlrichs' def2-TZVP basis set[82] and an effective core potential (ECP) for gold.[95] The default "NormalPNO" DLPNO settings were used as recommended for obtaining a reasonable balance between computational cost and accuracy.[96] The computational protocol for the combined DFT geometry optimizations and *ab-initio* single-point energy calculations is hereafter labeled as "DLPNO-CCSD(T)/def2-TZVP//BP86/TZ2P". This setup has also been used for the application of the Activation Strain Model (also known as distortion/interaction analysis) [97–99] to the dual σ,π gold-catalyzed Bergman cyclization of enediyne.

Results and discussion

1. Bonding features of the NHC-Au(I)-CCH complexes

In this section we aim to characterize the Au-CCH bond in the series of the NHCs-Au-CCH complexes (Scheme 1). In particular, we provide a quantitative assessment of the Dewar-Chatt-Duncanson (DCD) bonding components and their tuning by the different electronic properties of the considered NHC ancillary ligands.

Our calculations give interaction energies between $[NHC\text{-}Au]^+$ and $[CCH]^-$ fragments ranging from 172.6 to 208.6 kcal/mol, for the **6a**-Au-CCH and **3a**-Au-CCH complex, respectively (see Table 2). These energies are significantly larger than those reported[16] for gold-acetylide compounds bearing halogen atoms ($X=F^-$, Cl^-, Br^-, I^-) as ancillary ligands ($[X\text{-}Au(I)\text{-}CCH]^-$).

In Figure 1 the NOCV deformation densities and the corresponding Charge Displacement (CD-NOCV) curves for complex 1-Au(I)-CCH are shown as an illustrative example. The CD-NOCV analysis for all the other complexes can be found in the Supporting Information (Figures S2-S16). The numerical results of the *CT* values extracted from these CD-NOCV functions are reported in Table 1. From a qualitative perspective, all the NHC-Au-CCH complexes show the same bonding features. The CD-NOCV curve associated with the total deformation density ($\Delta\rho'$) is positive in the whole molecular complex (grey positive curve in Figure 1 for the 1-Au(I)-CCH complex) and shows that, overall, upon formation of the [NHC-Au]-CCH bond, a significant net charge transfer (CT_{net}) of 0.312 e occurs from the alkynyl ligand towards the metal fragment. As reported in Table 1, CT_{net} values span a range of about 0.1 electrons (0.301-0.390 e).

10.1002/ejic.202100260

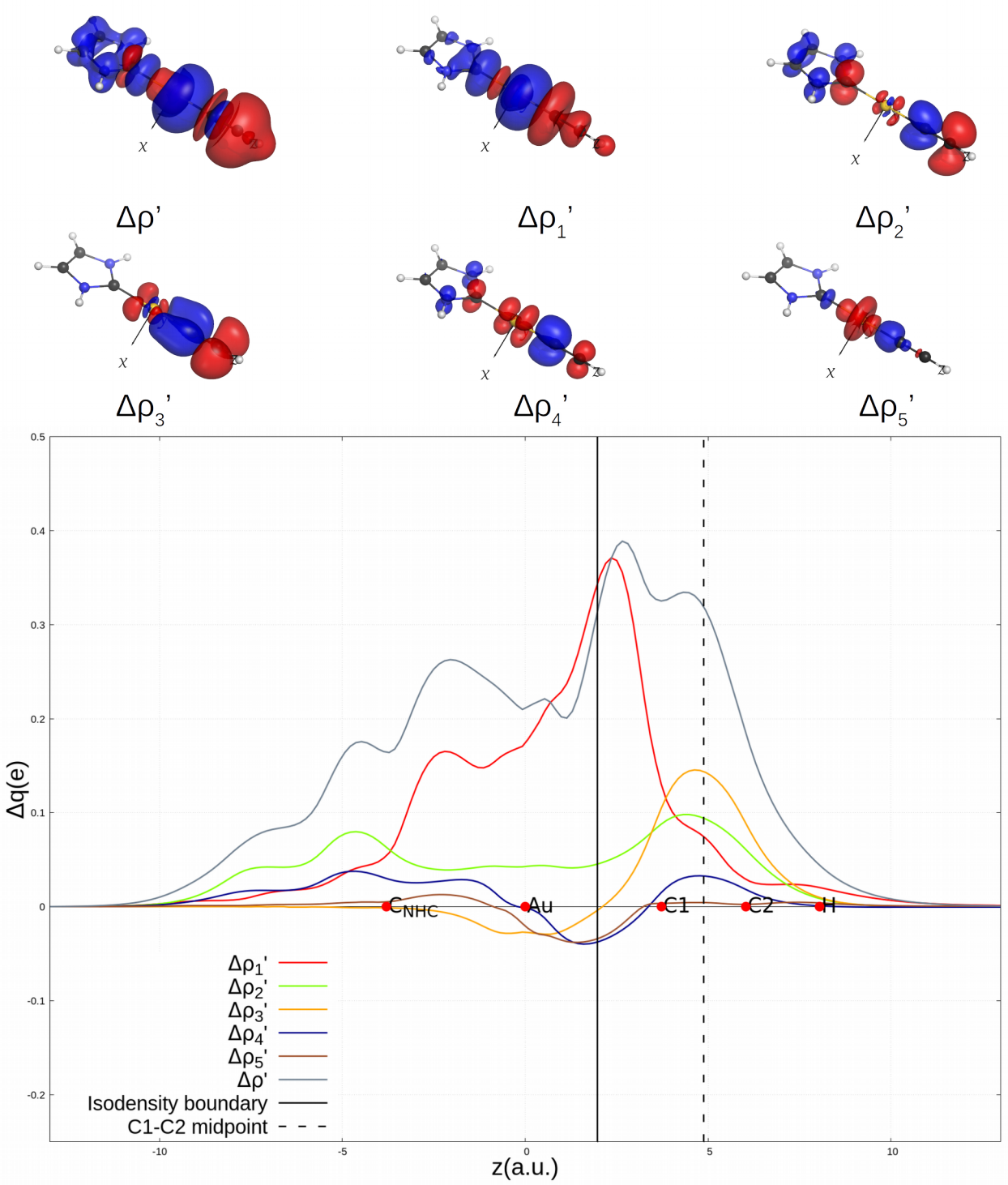

Figure 1. *Top:* Isodensity surfaces of the total (*Δρ'*) and the first five NOCV deformation densities (*Δρ$_1$' – Δρ$_5$'*) for the **1**-Au(I)-CCH complex. The isovalue for all the surfaces is ±0.001 e a.u.$^{-3}$. Blue regions indicate electron density accumulation areas, whereas red regions indicate depletion areas.
Bottom: Corresponding CD-NOCV curves for the **1**-Au(I)-CCH complex. Red dots indicate the position of the nuclei along the z axis. The vertical solid line marks the isodensity boundary between **1**-Au(I) and alkynyl fragments (see text for details), whereas the dashed line represents the midpoint of the C1-C2 bond. Distances are reported in atomic units.

10.1002/ejic.202100260

NHC	CT_{net} (e)	CT_1 (e)	CT_2 (e)	CT_3 (e)	CT_4 (e)	CT_5 (e)	CT_2^{midp} (e)	CT_3^{midp} (e)	CT_4^{midp} (e)	$CT_{(2+4)}^{midp}$ (e)
1	0.312	0.343	0.045	-0.004	-0.037	-0.034	0.094	0.144	0.004	0.098
2a	0.311	0.344	0.042	-0.004	-0.032	-0.033	0.092	0.143	0.032	0.124
2b	0.308	0.340	0.046	-0.011	-0.038	-0.033	0.084	0.135	0.039	0.123
2c	0.301	0.345	0.040	-0.019	-0.037	-0.034	0.101	0.127	0.020	0.121
2d	0.309	0.343	0.041	-0.005	-0.038	-0.033	0.093	0.142	0.029	0.122
2e	0.318	0.347	0.043	-0.008	-0.035	-0.031	0.108	0.138	0.016	0.124
2f	0.313	0.344	0.047	-0.008	-0.038	-0.033	0.071	0.137	0.056	0.127
3a	0.390	0.342	0.121	-0.002	-0.037	-0.034	0.149	0.146	0.036	0.185
3b	0.371	0.341	0.107	-0.009	-0.036	-0.033	0.136	0.136	0.036	0.172
3c	0.344	0.345	0.079	-0.014	-0.036	-0.032	0.117	0.131	0.034	0.151
3d	0.325	0.347	0.057	-0.014	-0.036	-0.031	0.114	0.130	0.020	0.134
4	0.321	0.344	0.046	-0.004	-0.036	-0.032	0.057	0.142	0.073	0.130
5	0.312	0.342	0.041	-0.008	-0.031	-0.034	0.128	0.140	-0.001	0.139
6a	0.331	0.349	0.052	-0.014	-0.032	-0.028	0.128	0.132	0.007	0.135
6b	0.326	0.344	0.054	-0.012	-0.033	-0.028	0.121	0.133	0.013	0.134
7	0.324	0.346	0.054	-0.007	-0.038	-0.028	0.076	0.139	0.055	0.131

Table 1. Charge transfer values calculated at the isodensity boundary of the CD-NOCV curves corresponding to the total (CT_{net}) and the first five NOCVs (CT_k) for all the NHC-Au(I)-CCH complexes. The charge transfer values evaluated at the midpoint of the C1-C2 bond (CT_k^{midp}) are also reported.

From inspection of the CD-NOCV curves and the isodensity pictures associated to the different NOCV deformation densities, we can immediately see that the most important contribution ($\Delta\rho_1$') is the σ donation from the alkynyl ligand towards the metal fragment. The CD-NOCV curve (red CD-NOCV curve in Figure 1) is positive in the whole molecular region and it is the most important contribution to the Au-CCH bond. At the isoboundary the charge transfer value (CT_1) amounts to 0.343 e, slightly larger than CT_{net}. The CD-NOCV pattern, which shows a large slope in the region around C1, suggests that the main contribution to *CT* comes from the lone-pair of $[CCH]^-$, mainly localized at C1. Surprisingly, from Table 1, we can see that the structural modifications introduced on the ancillary NHC ligands do not change the extent of this bond component, which varies only slightly along the series in the range 0.340/0.349 e.

The second most important contribution (NOCV deformation density labeled as $\Delta\rho_2$' in Figure 1) can be described as a charge rearrangement of π symmetry. It is associated to a CD-NOCV curve that is positive all over the molecular region, thus indicating that a net charge transfer *CT* from alkynyl towards the metal fragment occurs. The CD-NOCV curve associated to this component also highlights the presence of a direct π communication between the alkynyl ligand, which in this case behaves as a π-donor, and the NHC, which acts as a π-acceptor. It is intriguing to note that the gold center acts as a spectator, as indicated by the very small electron density rearrangement on the gold site and the almost flat CD-NOCV curve in this region.

The observed pattern is consistent with the well-recognized π-acceptor properties of NHCs and inspection of the isodensity surfaces ($\Delta\rho_2$' in Figure 1, top) clearly confirms this picture. Depletion areas on the C2 atom of the alkynyl ligand and on the C atom of the NHC (C_{NHC}) resemble the shape of p orbitals perpendicular to the NHC plane, resulting in large charge accumulation areas on the two nitrogen atoms and the π system of NHC. Interestingly, in contrast to the σ donation discussed above, this component is modulated by the structural modifications of the NHCs (see Table 1). These modifications cause a sizable variation of the π donation component, which spans a range of 0.081 e (0.04/0.121 e). Actually, this is the only component that is significantly modified along the complexes series. This finding is quantitatively demonstrated in Figure S17 in the SI, where a tight correlation between the CT_{net} and *CT* values associated to the π donation component (CT_2) is shown.

The remaining components give a smaller contribution to the bond in terms of *CT* between fragments. The $\Delta\rho_3$' and $\Delta\rho_4$' components (yellow and blue curves respectively in Figure 1)

can be easily discussed on the basis of the Dewar-Chatt-Duncanson model. They correspond to π back-donation components: *Δρ₃'* represents the component lying in the plane of the NHC ($\pi^{\parallel}$), whereas *Δρ₄'* is perpendicular with respect to the NHC plane ($\pi^{\perp}$). In both cases they show a clear depletion at the gold site and the corresponding CD-NOCV curves assume negative values in the region of gold, thus indicating a charge flux from Au towards the alkynyl. It is remarkable that both curves, as shown in Figure 1, assume positive values in the region of the alkynyl ligand (i.e. between C1 and C2 atoms) with a typical bell shape, which can be seen as the fingerprint for a strong polarization of triple bond with electron charge being shifted from the C2 to the C1 atom. This pattern indicates that the *Δρ₃'* and *Δρ₄'* components represent the π back-donation component combined with the polarization of the π electron density of the alkynyl ligand induced by the positively charged metal fragment, which shifts electron charge in the opposite direction. In the case of *Δρ₃'* (parallel in-plane π component) the polarization at the alkynyl is so large that almost perfectly balances the back-donation flux, resulting in a very small *CT* (CT_3 is equal to -0.004 e).[56,60] Within the whole series of complexes (Table 1) for both back-donation components, we observe small values of *CT* and very narrow variability ranges (CT_3 and CT_4 values vary in the range -0.019/-0.002 e and -0.031/-0.038 e, respectively).

A more quantitative measure of the charge shift involved in the π polarization mechanism may be given by evaluating the CD-NOCV functions at the midpoint of the alkynyl CC bond. We mention that a similar approach has been previously used to rationalize the π polarization and CO stretching frequency of classical and non-classical transition metal carbonyls (including gold(I) and gold(III) carbonyl complexes).[56,60] The results are also reported in Table 1. The contributions are shown separately according to the shape of the charge accumulation/depletion areas for the π back-donation and π donation components, namely the parallel contribution (CT_3^{midp}) and the perpendicular contributions (CT_2^{midp} and CT_4^{midp}). While the former shows a variation by 0.02 e ca. (range: 0.127/0.146 e), the latter, particularly when evaluated as global π perpendicular polarization ($CT_{(2+4)}^{midp}$), shows, analogously to the π donation component, a large variability (0.098/0.185 e).

Finally, the *Δρ₅'* component cannot be ascribed to any component of the DCD bonding model and does not show any polarization contribution in the CC region of the alkynyl site. The test results carried out by using an hybrid functional (Table S1 and Figure S1 in the SI) clearly rule out possible artificial effects due to the exchange-correlation functional (with this component being qualitatively and quantitatively unchanged upon change of the functional). Thus, this

component can be envisaged as a σ back-donation from the metal fragment towards the alkynyl and it varies in a very small range along the complexes series (-0.029/-0.034 e). This component has been previously observed for several transition metal complexes.[100,101]

2. Structure/bonding relationship

In this section, for the purpose of ligand design in gold catalysis, the different structural modifications of the NHCs will be related to the variation of the bonding properties, particularly focusing on the π donation component which we have found to be the most tunable component of the Au-alkynyl bond.

In Scheme 1, the different NHCs are grouped according to the different structural modifications of the carbene backbone with respect to the **1** ligand, which is taken as reference. Concerning NHCs **2a**-**2f**, we provided a symmetric substitution on the nitrogen atoms of the NHC, using different alkyl and aryl groups. These substituents (methyl, mesityl, tert-butyl, isopropyl, 2,6-diisopropylphenyl and phenyl) behave as electron-donating groups (EDGs), thus making the NHC moiety (and, in particular the C_{NHC} atom) not particularly prone to receive electron density from the alkynyl group. Our CD-NOCV results show indeed that these modifications have no remarkable consequences on the Au-C bond, since we observe only negligible variations with NHCs **2a**-**2f** of the tunable π donation component (CT_2 values are in the range 0.040/0.047 e) and no significant difference with the reference **1**-Au-CCH complex (CT_2=0.045 e).

A very similar situation occurs upon addition of a phenyl ring (complex **4**-Au-CCH) and saturation of the NHC backbone (complex **5**-Au-CCH): the extent of the π donation in these systems is comparable to that in the NHCs **1**-**2f** (CT_2 is 0.046 and 0.041 e for complexes **4**- and **5**-Au-CCH, respectively). In Figure S12 in the SI, the isodensity picture of complex **4**-Au-CCH shows an involvement of the aromatic π system in the delocalization of electron charge from the alkynyl, which, however, has no direct impact on the Au-alkynyl bonding properties.

Significant variations of the bonding properties are observed for NHCs **3a-3d**. In these four complexes, we changed the NHC backbone by adding oxygen atoms and varying both the groups attached to the nitrogen atoms and the size of the ring.

As already mentioned, the complex **3a**-Au-CCH shows a significant enhancement of the π-accepting properties of the carbene which, in this case, is able to increase π acidity of the metal fragment and to modulate the Au-alkynyl bond. The amount of the π donation in complex **3a**-Au-CCH is about three times as large as that reported for complex **1**-Au-CCH (0.121 vs 0.045 e, respectively), whereas the remaining *CT* values are very similar, thus being responsible for the huge variation of the CT_{net} value (0.390 vs. 0.312 e, respectively) which can be ascribed to the variation of the extent of the π donation. This behavior has been

previously attributed to the capacity of the two oxygen atoms of accepting π electron charge through mesomeric effect.[37] The increased π donation causes the perpendicular π polarization ($CT_{(2+4)}^{midp}$ in Table 1) also to increase (0.185 e for complex **3a**-Au-CCH vs 0.098 e for complex **1**-Au-CCH).

The replacement of the hydrogen atoms with electron-donating mesityl groups as substituents on the nitrogen atoms of the NHC allows for modulation and quenching of the π-acceptor properties of the carbene, as shown by the results obtained for complex **3b**-Au-CCH, showing that the amount of π donation is slightly reduced (0.107 e). This trend could be expected on the basis of what we mentioned previously for EDGs: the ability of the mesityl group to donate electron charge to the carbene quenches the ability of the C_{NHC} atom of accepting electron charge from the alkynyl, thus making the π communication between these two ligands slightly less effective.

The π-acceptor properties of **3b** are sizably reduced by the insertion of a carbon atom separating the two oxygens, namely by enlarging the ring to a six-membered ring (ligand **3c**), where the extent of π donation is reduced by almost 30% (0.079 e). This finding could also be expected for two different reasons: i) the six-membered ring loses the planarity of **3a** and **3b**, thus causing the π communication to be less effective; ii) the two methyl groups between the two oxygen atoms contribute (since they behave as weak EDGs) to make the carbene C_{NHC} atom less prone to accept the alkynyl's π donation.

Further decrease of the π-acceptor ability of the carbene is observed when one of the oxygen atoms is removed from the six-membered cycle, as in complex **3d**-Au-CCH. In this case, removal of an oxygen atom (which is responsible for the enhanced π acceptor properties of the NHC) provides an even more decreased π communication, with an associated *CT* value of 0.057 e. It is worth noting that in this "transition" from NHC **3a** to **3d**, where we imposed an increasing number of structural modifications causing the π communication to be quenched, the π donation in complex **3d**-Au-CCH (i.e. the "most quenched") is still larger (more than 0.01 e) than that observed for NHCs **1**, **2a-f**, **4** and **5**.

Finally, we modify the backbone of NHC by substituting one of the nitrogen atoms with different heteroatoms, (i.e. a carbon atom for NHCs **6a-6b** and a sulfur atom for complex **7**-Au-CCH). We see that these structural modifications only slightly affect the bond, since complexes **6a**-, **6b**- and **7**-Au-CCH show a slightly enhanced π donation with respect to the lowest π-accepting NHC complexes (CT_2 values are 0.052, 0.054 and 0.054 e, respectively). The explanation for such enhancement lies on the fact that the carbon and sulfur atoms in

these complexes are not able to donate π electron charge to the C_{NHC} carbon atom, thus enhancing its ability to accept π density from the trans alkynyl ligand. However, in all the three cases, large EDGs are present on the carbene ring that are responsible, via inductive effect, for enhancing the carbene electron charge, making it less π acid. It is worth noting that, again, the presence of the phenyl ring fused on the NHC backbone in complex **7**-Au-CCH shows no improvement of its π-accepting properties, which is consistent with the low aromaticity of these species.

For completeness, in Table 2 the results of the Energy Decomposition Analysis (EDA) are presented, where the orbital interaction (ΔE_{oi}) term, which accounts for the energy contribution of covalent and polarization interactions between fragments, can be decomposed via ETS-NOCV framework according to the contributions of the single NOCVs. The contribution of dispersion to the overall interaction energy is reported in Table S2 in the SI and it is shown to be quite small for all the complexes (generally less than 4 kcal/mol) and to display no peculiar trends along the series.

NHC	ΔE	ΔE^{Pauli}	ΔV_{elst}	ΔE_{oi}	ΔE_{oi}^{1}	ΔE_{oi}^{2}	ΔE_{oi}^{3}	ΔE_{oi}^{4}	ΔE_{oi}^{5}
1	-188.1	227.1	-327.0	-88.2	-51.1	-7.4	-8.4	-7.0	-7.0
2a	-184.5	227.8	-323.7	-88.6	-51.3	-7.0	-8.2	-7.0	-7.1
2b	-176.1	226.7	-313.5	-89.2	-50.1	-6.6	-7.7	-7.0	-7.1
2c	-177.5	228.7	-317.9	-88.3	-50.3	-6.6	-7.8	-6.8	-7.5
2d	-180.8	227.9	-319.9	-88.9	-51.0	-6.7	-8.0	-6.9	-7.1
2e	-176.2	229.3	-313.0	-92.5	-51.4	-6.9	-7.7	-6.5	-7.5
2f	-180.1	228.6	-318.5	-90.1	-50.6	-6.9	-7.9	-7.4	-7.3
3a	-208.6	235.2	-345.2	-98.6	-54.2	-14.3	-9.4	-6.5	-7.6
3b	-190.5	234.5	-327.0	-98.1	-53.5	-11.9	-8.3	-6.4	-8.1
3c	-182.4	233.1	-320.3	-95.2	-52.4	-9.3	-8.0	-6.5	-7.8
3d	-176.3	231.7	-314.9	-93.1	-52.5	-7.5	-7.7	-6.2	-7.8
4	-181.4	228.5	-318.8	-91.1	-51.3	-7.5	-8.0	-7.6	-7.2
5	-186.1	227.7	-325.9	-87.9	-51.6	-7.9	-8.4	-5.7	-7.1
6a	-172.6	232.6	-310.7	-94.5	-53.3	-7.6	-7.6	-5.6	-7.7
6b	-172.7	230.5	-310.3	-92.9	-52.8	-7.6	-7.6	-5.8	-7.6
7	-177.1	229.8	-314.5	-92.4	-51.7	-7.5	-7.9	-7.3	-7.2

Table 2. Results of the EDA analysis for the series of 16 NHC-Au(I)-CCH complexes. From the left to the right:

interaction energy (ΔE), Pauli repulsion (ΔE^{Pauli}), electrostatic interaction (ΔV_{elst}), orbital interaction (ΔE_{oi}) and contributions of the first five NOCVs to the orbital interaction (ΔE_{oi}^{1}, ΔE_{oi}^{2}, ΔE_{oi}^{3}, ΔE_{oi}^{4}, ΔE_{oi}^{5}). All energies are in kcal/mol.

The EDA shows that the electrostatic contribution (ΔV_{elst}) to the interaction energy has an important role in determining such a strong Au-C interaction, since the two interacting fragments ($[NHC\text{-}Au]^{+}$ and $[CCH]^{-}$) bear a positive and a negative charge, respectively. ΔV_{elst} value overcomes in all cases the repulsive Pauli interaction (ΔE^{Pauli}) and varies widely along the series (from -310.29 to -345.23 kcal/mol).

However, the orbital interaction (ΔE_{oi}) contribution to the bond is far from being negligible. In all cases, it provides a sizeable stabilization of the interaction energy and, on average, it represents almost the 50% of the latter. We observe a variation of the ΔE_{oi} by 10 kcal/mol ca. along the series that, in most cases, can be ascribed to the variations observed for the π donation. We can see that the ΔE_{oi} associated to NOCVs 1, 3, 4 and 5 changes only negligibly along the series. The most variable component is, again, the π donation (NOCV 2). It can be observed that for the best π acceptor NHCs identified via CD-NOCV analysis (i.e. **3a** and **3b**), a high interaction energy is calculated (-208.6 and -190.5 kcal/mol, respectively). Here, the ΔE_{oi} term is very high (-98.6 and -98.1 kcal/mol, respectively) and the contribution of the π donation to it (ΔE_{oi}^{2}) is twice as large as that for the other NHCs (-14.3 and -11.9 kcal/mol, respectively, whereas for other complexes is, on average ca. 7 kcal/mol). It is interesting to note that there is a significant qualitative difference between the relative importance of the NOCV-pair contributions to the charge transfer and the corresponding contributions in terms of interaction energy. The explanation for these differences lies in the fact that the energy contributions are more accurately related to the overall density rearrangement across the whole molecular system described by the corresponding NOCV density deformation component, while the *CT* charges are only related to the CD-NOCV function value in the interfragment region.

3. Experimental observables/bonding features relationship

In the previous section we have demonstrated that the most important modifications at the gold-alkynyl bond involve the tuning of the π acidity of the metal fragment which results in a direct π communication between the alkynyl and the NHC ancillary ligands.

In this section we investigate whether this intriguing bonding pattern may be revealed by some experimental observables. As also mentioned in the Introduction, the Charge Displacement analysis was already successfully employed for this purpose, in different contexts, including gold complexes. [56,59–62,102] It was found to be a useful tool to single out specific correlations between bonding features and experimentally measurable parameters.

In Table 3 we present the most relevant structural and spectroscopic parameters for the NHC-Au(I)-CCH complexes series. The C1-C2 bond lengths and stretching frequencies vary only negligibly along the series (in the ranges of 0.001 Å and 13 cm^{-1}, respectively) and these small variations do not follow any trend.

NHC	r_{C1-C2} (Å)	r_{Au-C1} (Å)	r_{NHC-Au} (Å)	$\tilde{\nu}_{C1-C2}$ (cm^{-1})	$\Delta\sigma_{iso}^{C1}$ (ppm)	$\Delta\sigma_{iso}^{C2}$ (ppm)
1	1.222	1.969	2.008	2023.3	0.00	0.00
2a	1.222	1.971	2.022	2022.4	-1.49	-0.07
2b	1.222	1.972	2.008	2020.2	-0.76	0.65
2c	1.222	1.972	2.036	2023.1	4.42	-0.70
2d	1.222	1.971	2.021	2020.8	-1.65	-0.11
2e	1.222	1.972	2.011	2023.8	2.04	-1.64
2f	1.222	1.970	2.020	2022.6	1.02	-0.22
3a	1.223	1.961	1.980	2014.2	-5.10	-19.68
3b	1.223	1.981	1.967	2011.7	-4.74	-15.94
3c	1.222	1.967	2.009	2016.9	1.37	-8.76
3d	1.222	1.971	2.020	2019.6	2.28	-2.92
4	1.222	1.971	2.019	2021.2	-1.61	-1.70
5	1.222	1.970	2.012	2024.7	-0.46	0.03
6a	1.222	1.977	2.015	2020.6	3.35	-4.72
6b	1.223	1.979	2.006	2017.6	-1.25	-5.53
7	1.222	1.970	2.004	2021.1	2.37	-3.90

Table 3. Calculated structural and spectroscopic parameters for the NHC-Au(I)-CCH complexes series. From the left to the right: bond distance between C1 and C2 atoms of the alkynyl (r_{C1-C2}), bond distance between gold and

the alkynyl C1 atom (r_{Au-C1}), bond distance between gold and the carbene C_{NHC} atom (r_{Au-NHC}), stretching frequency of the alkynyl bond ($\tilde{\nu}_{C1-C2}$) and the total isotropic NMR shielding for the C1 ($\Delta\sigma_{iso}^{C1}$) and the C2 ($\Delta\sigma_{iso}^{C2}$) atoms of the alkynyl ligand. The isotropic NMR shieldings have been shifted with respect to complex **1**-Au-CCH value taken as zero reference (σ_{iso}^{C1} = 66.20 ppm; σ_{iso}^{C2} = 96.32 ppm).

The most remarkable variations can be found for the Au-C1 and C_{NHC}-Au bond lengths (in the ranges of 0.02 and 0.06 Å, respectively). In particular, the C_{NHC}-Au bond lengths reveal a qualitative correlation with both CT_{net} and CT_2 (i.e. the *CT* associated to the π donation) values (see Figure S18 in the SI). The trend indicates that stronger π-acceptor NHCs (and therefore higher values of *CT*) correspond to shorter Au-C_{NHC} bonds, which is consistent, since larger *CT* can be associated to a more covalent character of the bond and therefore to a shorter Au-C_{NHC} bond length. However, this correlation has only a qualitative character (R^2=0.72), thus suggesting that the structural variations are likely affected by other factors (electrostatic interactions, for instance).

At this stage it is worth exploring the potentialities of the ^{13}C NMR spectroscopy for monitoring the gold-alkynyl bond modulation. This technique has been used several times as a useful tool for evaluating the electronic properties of the NHCs[20] and, in the framework of gold complexes, it has been found to be suitable for selectively probing the σ donation[61,62] or π back-donation[59] of the DCD bonding model. It has been also suggested that the electronic properties (and in particular the π-accepting power) of NHC-metal compounds could be efficiently probed via NMR spectroscopy.[103] Moreover, some of us have recently demonstrated that the extent of the π communication in gold(I) diarylallenylidene compounds tightly correlates with the experimental ^{13}C NMR chemical shifts.[58] In the present case, NMR ^{13}C chemical shifts of the two carbon atoms of the alkynyl may be in principle shielded and deshielded by different bonding mechanisms and in particular by the π communication between the alkynyl ligand and the metal fragment. The π donation component possesses two essential features: i) an increase of π communication extent causes, in principle, the two carbon atoms to be deshielded and ii) π communication shows a variability along the series, suggesting that for the complexes with larger π donation an appreciable deshielding on the two carbon atoms should be observed.

We have seen that the electron density rearrangement at the two carbon atoms is intimately connected by the presence of both the π alkynyl-to-metal donation and the π polarization which, as discussed above, shifts charge from the C2 to the C1 atom. This means that, in the

case of the C2 atom, π polarization and π donation play accordingly, causing an overall removal of electron charge from this atom. On the other hand, for the C1 atom, these two charge rearrangements, providing charge accumulation/depletion patterns, may be harder to be experimentally disentangled. This pattern can be clearly observed in Figure 1 where the CD-NOCV curve representing the total electron rearrangement ($\Delta\rho'$) shows a large positive value that increases in the region around the C2 and nuclei positions (charge depletion) taking a value of 0.3 e (evaluated at the mid-point of the C1-C2 bond), while the CD-NOCV curve remains relatively flat at the C1 region.

The calculated NMR isotropic chemical shielding constant ($\Delta\sigma_{iso}$) are reported in Table 3. As shown in Figure S19 in the SI, the $\Delta\sigma_{iso}$ values for the C1 atom does not correlate with neither the CT_2 nor the CT_{net} values for this series of complexes, because of the complicated patterns of charge accumulation and depletion on this atom. Concerning the C2 atom, instead, the calculated $\Delta\sigma_{iso}$ very nicely correlates with both CT_2 and the CT_{net} values, as shown in Figure 2. This correlation, combined with the Au-alkynyl bonding model given by the CD-NOCV analysis, allows to build a model that bridges theory and experimental observables for this class of gold complexes: modification at the NHC site can be used to tune the π-accepting ability of the metal fragment and the latter may be revealed by the ^{13}C NMR spectroscopy at the C2 carbon of the alkynyl site.

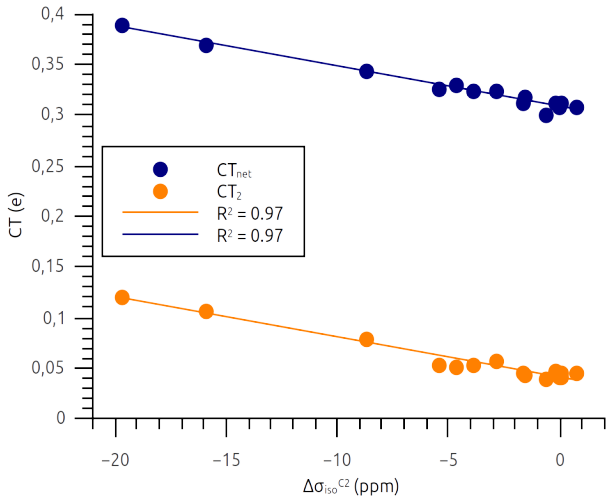

Figure 2. Correlation plot between the calculated total isotropic NMR shieldings for the C2 atom of the alkynyl ligand and the charge transfer corresponding to the π donation component (CT_2) and to the overall net charge transfer (CT_{net}).

One may advocate that this tight relationship between bonding features and experimental observables is somehow biased, since we are dealing with gold-acetylide complexes (NHC-Au-CCH), whereas, usually, stable gold-alkynyl complexes feature a more conjugated ligand, with alkyl or aryl R groups replacing the terminal hydrogen (NHC-Au-CCR). With the aim of extending the model, we substitute the acetylide anion with the phenylethynyl anion (i.e. substitution of a terminal hydrogen with a phenyl group). As the ligands, we use two NHCs that, according to our analysis, have a remarkably different trans effect on the Au-C bond (Scheme 2). Complex **2b**-Au-**Ph** has been recently synthesized and characterized via NMR spectroscopy,[40] while complex **3b**-Au-**Ph** has been obtained by substituting the NHC **2b** with **3b** (i.e. by simply replacing the hydrogens on the backbone of NHC **2b** with two oxygen atoms, thus enhancing its π-accepting power).

The results of the CD-NOCV analysis for complexes **2b**-Au-**Ph** and **3b**-Au-**Ph** are reported in the SI (Figures S20-S21 and Table S3). It has been found that the bonding scheme does not change upon substitution of the acetylide with the phenylethynyl: σ donation and all back-donation components are both qualitatively and quantitatively similar to those of the corresponding model acetylides. The only remarkable difference relies in the enhancement of the π donation of the alkynyl towards the metal fragment in **3b**-Au-**Ph**. The *CT* associated to this component, as also shown in Figure 3, varies substantially, with complex **3b**-Au-**Ph** having a *CT* value that is four times larger than that of complex **2b**-Au-**Ph** (0.167 and 0.038 e, respectively). The π donation in complex **3b**-Au-**Ph** is much larger than that of the corresponding acetylide (complex **3b**-Au-CCH), which may be surmised on the basis of the expected larger π donor ability of the phenylethynyl substrate. The results of the chemical shielding for the C1 and C2 atoms are reported in Table 4. Remarkably, the $\Delta\sigma_{iso}{}^{C1}$ and $\Delta\sigma_{iso}{}^{C2}$ values for phenylethynyl (3.9 and 16.6 ppm, respectively) complexes are consistent with those we found for acetylide (3.7 and 15.5 ppm, respectively). This result suggests that the ^{13}C NMR shielding constant of the C2 carbon at the alkynyl is a promising probe for the π acidity of a metal fragment. Clearly, it would be desirable to ascertain the generality of this spectroscopic/bond relationship by extending our investigation to other gold(I)-alkynyl complexes, including different alkynyls or ancillary ligands.

10.1002/ejic.202100260

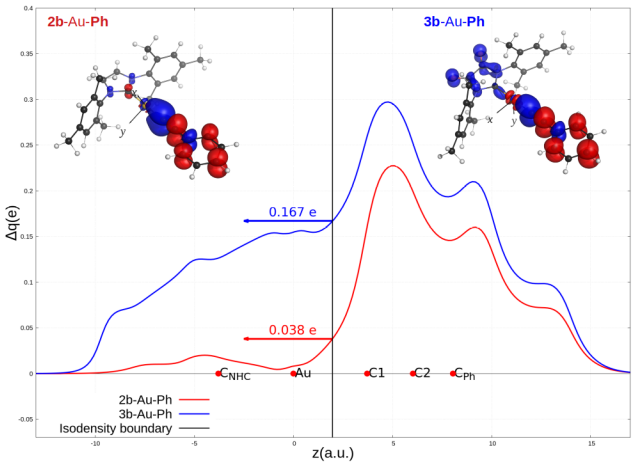

Figure 3. CD-NOCV curves of the π donation bond component for the **2b**-Au-**Ph** and **3b**-Au-**Ph** complexes. Red dots indicate the average position of the nuclei along the z axis. The vertical line marks the isodensity boundary between the NHCAu(I) and alkynyl fragments (see text for details). The arrows represent the charge transfer (*CT*) values for each complex evaluated at the isodensity boundary. The insets represent the isodensity surfaces of the π donation bond component for the **2b**-Au-**Ph** and **3b**-Au-**Ph** complexes. The isovalue for all the surfaces is ±0.001 e a.u.$^{-3}$. Blue regions indicate electron density accumulation areas, whereas red regions indicate depletion areas.

Complex	σ_{iso}^{C1} (ppm)	σ_{iso}^{C2} (ppm)	$\Delta\sigma_{iso}'^{C1}$ (ppm)	$\Delta\sigma_{iso}'^{C2}$ (ppm)
2b-Au-**Ph**	47.1	81.8	3.7	15.5
3b-Au-**Ph**	43.4	66.3		
2b-Au-CCH	65.4	97.0	3.9	16.6
3b-Au-CCH	61.5	80.4		

Table 4. Calculated isotropic chemical shieldings of the C1 and C2 atoms (σ_{iso}^{C1} and σ_{iso}^{C2}) for complexes **3b**-Au-**Ph**, **3b**-Au-**Ph**, **2b**-Au-CCH and **3b**-Au-CCH. The difference between chemical shieldings $\Delta\sigma_{iso}'$ ($\Delta\sigma_{iso}' = \sigma_{iso}$(***2b***-*Au*-***Ph***) – σ_{iso}(***3b***-*Au*-***Ph***)) has been also reported.

4. Structure/reactivity relationship: a case study in the dual gold catalysis

It has been already mentioned in the Introduction that Au(I) complexes behave as versatile catalysts in several types of reactions, among which processes featuring an alkynyl moiety with η^1 coordination to gold, such as in the dual-activation catalysis, are becoming increasingly popular.[11,12]

The use of gold catalysts in cycloaromatization reactions,[104] which represents one of the main approaches for the formation of cyclic structures in organic chemistry, has been recently object of an in-depth computational study by Alabugin et al.[14] The study focused on the effect of gold catalysis in the Bergman cyclization (BC) and also discussed the effect of the dual-catalysis mode on such reaction (Scheme 3), showing that it may provide further acceleration of the process with respect to mono-gold catalysis and an improved thermodynamical stabilization of the product. By relying on an ad-hoc formulation of the Activation Strain Model[97] (or, as they refer to, “distortion/interaction analysis”), they point out that the improved efficiency of the dual-catalytic mode is mainly due to a reduced strain penalty that favors a more stable transition state. They showed that the additional gold moiety is able to efficiently stabilize the positive charge on the C5 carbon atom (β-position) of the product, thus improving its thermodynamic stability. The study also provides a solid theoretical framework for understanding the nature of the catalytic effects including possible effects of the ancillary ligands on the two gold moieties. The authors used trimethylphosphine (PMe_3) as the ancillary ligand for the reactivity model they present. In this context, our aim is to investigate whether the structural modifications on the backbone of the NHC ligand in the η^1-coordinated gold is able to affect the catalytic process. In order to isolate the electronic effect of the NHC structure on the gold-carbon σ bond, we model the reaction using the PMe_3 ligand for the η^2-coordinated gold moiety ($[Au(PMe_3)]^+$), whereas we use NHCs **1** and **3a** for the gold-alkynyl moiety (Scheme 3), since, as discussed earlier, they present different electronic properties. We need to point out that, in order to try to isolate the effect of the NHC structure on the gold-carbon σ bond (and, as a consequence, on its role in the reaction), we only substitute one ligand to be able to disentangle the effects of the σ and the π coordination of gold. To avoid possible effects related to the steric hindrance of the ligands, we chose two NHCs that have a very similar steric hindrance (both ligands bear hydrogen atoms as substituents). It should be clear that we aim to get insights on this specific aspect of the reaction and we do not claim to be predictive for the whole reaction itself.

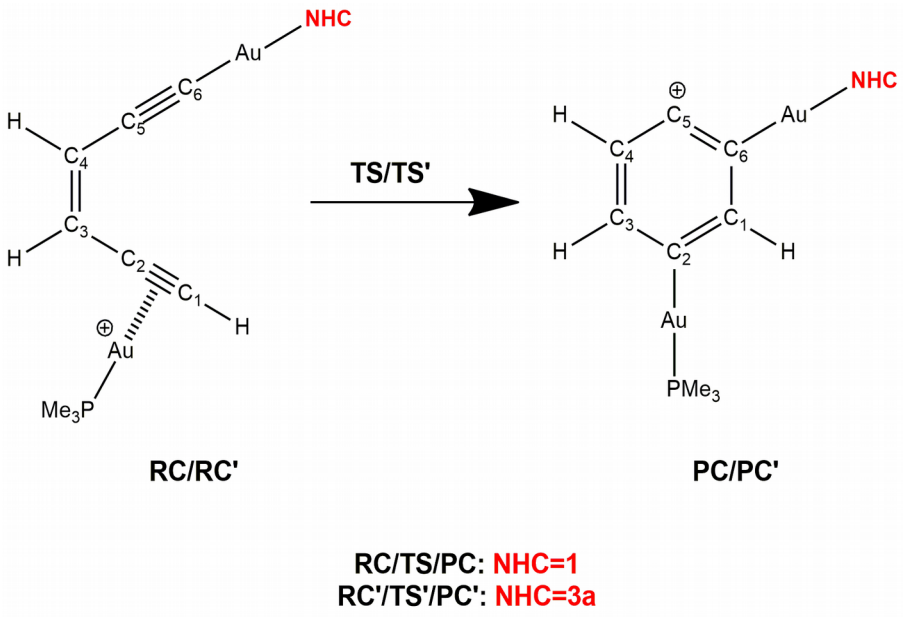

Scheme 3. Dual-gold-catalyzed Bergman cyclization (BC) where the NHC coordinated in an η^1 mode to the gold moiety has been changed according to its electronic properties (i.e. NHCs **1** and **3a**).

The energy profiles for the dual-catalyzed Bergman cyclization are reported in Figure 4. These results have been obtained in the gas phase (the solvent effect is systematic in the reaction profiles, see Figures S22-S23 in the SI). The energy profiles give a clear picture: upon substitution of NHC **1** with NHC **3a**, the activation barrier increases (5.6 and 8.2 kcal/mol for NHCs **1** and **3a,** respectively). This finding is even more interesting if we consider that the decrease in the activation barrier passing from the dual-Au mechanism to the mono-Au case found by Alabugin et al. is by 6.2 kcal/mol.[14] In other words, by only performing a structural modification of the NHC ancillary ligand in the η^1 moiety, we induced a change in the activation barrier that is more than 30% of the change found by introducing a second gold fragment in the catalytic process. The effect of the structural modification at the NHC site is even more noticeable thermodynamically: the product PC (-14.0 kcal/mol) is more stable than the product PC' (-10.2 kcal/mol). All these results clearly suggest that the modulation of the gold-carbon σ bond via structural modifications on the NHC ligand may be used to influence the overall reactivity in dual-gold-catalyzed cycloaromatization processes.

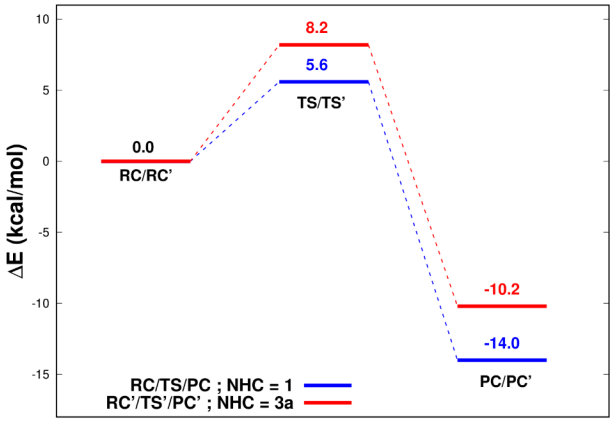

Figure 4. Energy profiles of the Bergman cyclization with different NHC groups coordinated to the gold-alkynyl moiety (**1**, **3a**). The calculations have been carried out at the DLPNO-CCSD(T)/def2-TZVP//BP86/TZ2P level (see Methodology section for further details). The **RC/RC'** energy is taken as zero reference point.

As mentioned above, Alabugin et al. used the Activation Strain Model (ASM, referred to as "distortion/interaction analysis) in order to get insights on the factors controlling the activation barrier. We recall that, within this framework, we can decompose the activation barrier ($\Delta E^{\#}$) of the process as follows:

$$\Delta E^{\#} = \left[\Delta E_{\text{dist}}(TS) - \Delta E_{dist}(RC)\right] + \left[\Delta E_{\text{int}}(TS) - \Delta E_{\text{int}}(RC)\right] = \Delta\Delta E_{dist} + \Delta\Delta E_{\text{int}} \quad [4]$$

where the "$\Delta E_{dist}(TS)$" and "$\Delta E_{dist}(RC)$" terms represent the energy penalty due to the distortion of the fragments (i.e. the substrate with the $[AuNHC]^+$ fragment coordinated in a η^1 mode and the $[AuPMe_3]$ fragment) constrained in the structures of the transition state (TS/TS') and the reactant (RC/RC') respectively, whereas "$\Delta E_{int}(TS)$" and "$\Delta E_{int}(RC)$" represent the interaction energies between the fragments (with the geometries constrained at the ones assumed in the TS/TS' and RC/RC' respectively) in the two structures. These terms can be grouped in the "$\Delta\Delta E_{dist}$" and "$\Delta\Delta E_{int}$" terms, that represent the overall distortion and interaction contributions to the activation barrier, respectively. The results of the analysis are reported in Table 5.

Energies (kcal/mol)	NHC	
	1	**3a**
ΔE_{dist} *(RC)*	5.5	4.7
ΔE_{dist} *(TS)*	18.0	20.2
$\Delta\Delta E_{dist}$	12.5	15.5
ΔE_{int} *(RC)*	-57.6	-52.0
ΔE_{int} *(TS)*	-64.5	-59.3
$\Delta\Delta E_{int}$	−6.9	-7.3
$\Delta E^{\#}$	5.6	8.2

Table 5. Results of the Activation Strain Model (ASM) approach for the Bergman cyclization with different NHC ligands (**1**,**3a**). In the last row the activation barriers ($\Delta E^{\#}$) are reported. The analysis has been carried out at the DLPNO-CCSD(T)/def2-TZVP//BP86/TZ2P level.

Upon substitution of the NHC ligand, the difference between the two activation barriers stems mainly from the reduced distortion penalty observed for the NHC ligand **1** with respect to NHC **3a**. Indeed, the $\Delta\Delta E_{int}$ values (i.e. the overall contribution to the activation barriers) are comparable between the two NHC groups, with $\Delta\Delta E_{int}$ being slightly favored for NHC **3a** (-7.3 kcal/mol) with respect to NHC **1** (-6.9 kcal/mol). The distortion penalty is the factor that really discriminates the two reaction paths: while the distortion referred to RC and RC' ($\Delta E_{dist}(RC)$) is slightly favored for NHC **3a** (4.7 vs. 5.5 kcal/mol), the penalty referred to TS and TS' ($\Delta E_{dist}(TS)$) is favored for NHC **1** (18.0 vs. 20.2 kcal/mol), thus making the overall distortion penalty ($\Delta\Delta E_{dist}$) smaller for NHC **1** (12.5 kcal/mol) with respect to NHC **3a** (15.5 kcal/mol), resulting in an overall lower activation barrier for NHC **1**.

In order to rationalize the reduction of the distortion penalty, it is useful to recall that the latter is due to electronic effects originating when the fragments are constrained into the final molecular geometries. It has been reported that, in some cycloaddition reactions, the reduction of the distortion penalty is often due to the increased hyperconjugative assistance that provides the stabilization of the transition state.[105–108] Alabugin et al.[14] found that lower distortion penalty in the (σ,π) dual Au(I) catalyzed reaction respect to Au-mono mechanism was given by considering the capability of the σ coordinated gold moiety to stabilize the forming positive charge on the C5 carbon atom.

In order to check whether such interpretative framework can also apply to our case, we

computed the Voronoi Deformation Density (VDD) charges for the C5 carbon atom for all the structures along the reaction profile. As reported in Figure 5a and 5b, where all the structures are shown as well as the VDD charges on the C5 atom, we see that in our case the trend is analogous: along the reaction path, the charge on the C5 atom is less positive (or more negative) when NHC **1** is used with respect to NHC **3a**. This trend is found for RC and RC' (-0.106 and -0.087 e, respectively), TS and TS' (-0.064 and -0.038 e, respectively) and, most importantly, for PC and PC', where, in the case of the former, a smaller positive charge on the C5 atom (+0.107 e) with respect to the latter (+0.118 e) is calculated.

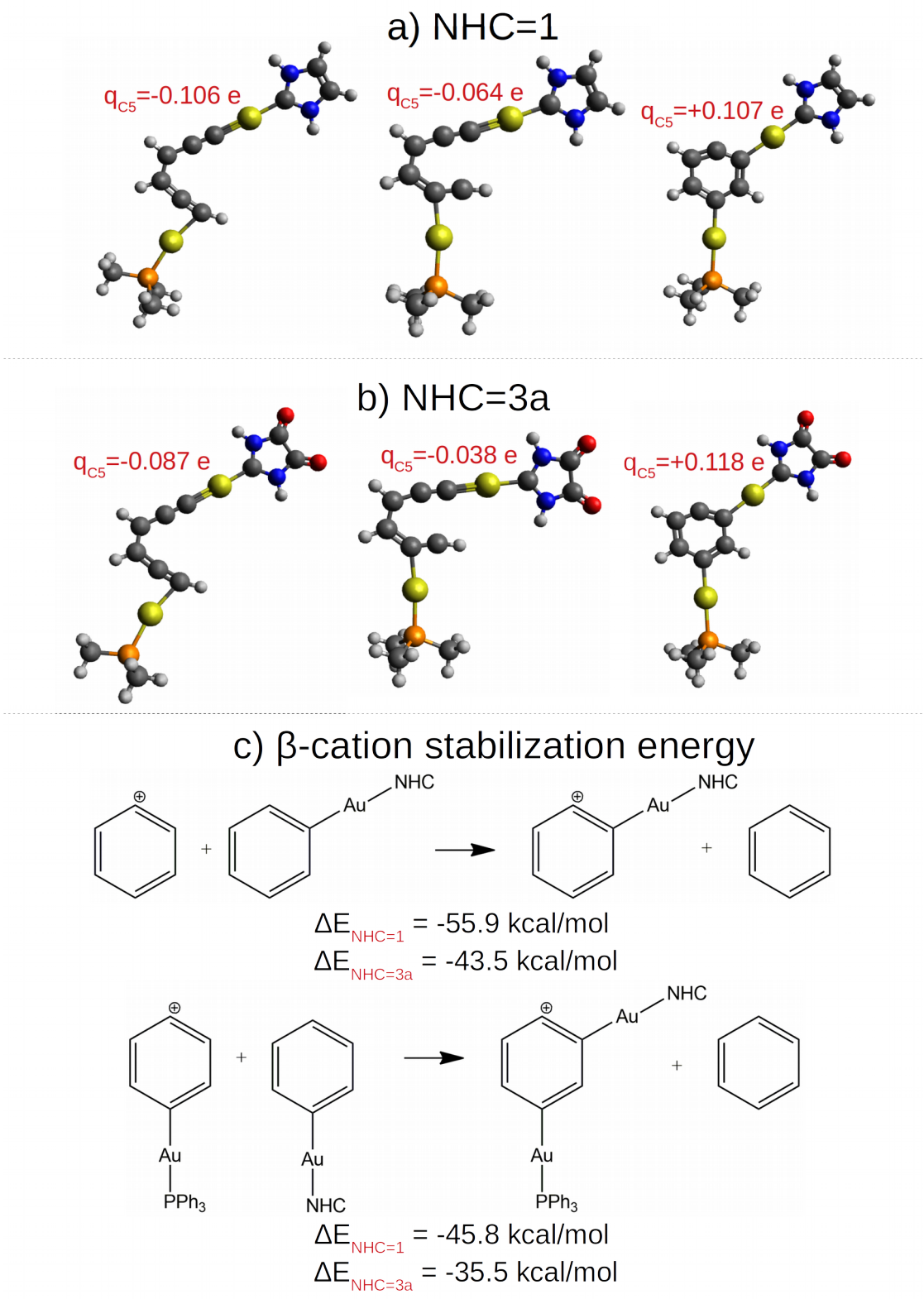

Figure 5. a) Structures (from left to right) of RC, TS and PC (NHC=**1**). The Voronoi Deformation Density (VDD) charges on the C5 atom calculated at the DLPNO-CCSD(T)/def2-TZVP//BP86/TZ2P are reported for all structures. **b)** Structures (from left to right) of RC', TS' and PC' (NHC=**3a**). The Voronoi Deformation Density (VDD) charges on the C5 atom calculated at the DLPNO-CCSD(T)/def2-TZVP//BP86/TZ2P level are reported for

all structures. **c)** β-cation stabilization energy of the two product complexes (PC and PC') with and without the $[AuPMe_3]^+$ fragment calculated at the DLPNO-CCSD(T)/def2-TZVP//BP86/TZ2P level.

The ability of the $[AuNHC]^+$ fragment to stabilize this positive charge on the product complex has been also quantitatively evaluated by calculating the β-cation stabilization energy (a similar approach has been also used in Ref. [14]), i.e. how much the phenyl cation is stabilized by the presence of an *ortho*-[AuNHC] fragment. As shown in Figure 5c, it is evident that NHC **1** provides a much stronger stabilization of the positive charge on the C5 atom (-55.9 kcal/mol) with respect to NHC **3a** (-43.5 kcal/mol) and this finding fits very nicely with the bonding model reported in the previous Sections. Indeed, we demonstrated that NHC **3a** is a much stronger π-acid that establishes a stronger π-communication with the unsaturated substrate and causes electron charge to be depleted from the neighboring η^1-coordinated alkynyl fragment. Therefore, it is clear that such a pattern would tend to decrease the electronic density at the C5 carbon atom providing a destabilization for the positive charge and, consequently, a higher activation barrier for the more acidic NHC **3a** with respect to NHC **1**. When the *para*-$[AuPMe_3]^+$ group is included, the stabilization is reduced but overall confirms that NHC **1** provides a greater stabilization of the positive charge (-45.8 kcal/mol) with respect to NHC **3a** (-35.5 kcal/mol).

In a much wider context of the dual-gold-catalyzed cycloaromatizations, the Bergman cyclization is the "parent" of 6-*endo* cyclizations that allow to form six-membered rings. However, the experimental characterization of such reactivity came later with respect to the dual-gold-catalyzed 5-*endo* pathways, in which, via a gold-vinylidene intermediate, five-memebered rings are formed.[11,109,110]The competition between the two patterns is far to be obvious. As an example, a joint experimental and theoretical study by Hashmi et al. shows that with increasing aromatic stabilization of the 6-*endo* product, the transition states for 5-*endo* and 6-*endo* cyclization shift closer together on the surface making an energetic distinction impossible (the 5-*endo* and 6-*endo* transition states have a calculated energy difference of 1.9 kcal/mol) and outcompeting classical transition-state theory.[111] Nonetheless, to the best of our knowledge, no study has been carried out concerning the effect of structure of the ancillary ligand on such selectivity. Of course, a quantitative and complete assessment of the ligand effect in this reactivity is far from the aim of this work. Nonetheless, our results, assessing the effect of the modified NHC ligand in the gold-alkynyl moiety, may pave the way for the modulation of the selectivity between 5- and 6-*endo* products. Indeed, we report here

that the NHC **3a** tends to destabilize the positive charge on the 6-*endo* product (and transition state), thus disfavoring the formation of the latter (e.g. in favor of a 5-*endo* cyclization) with respect to NHC **1**. In a much wider picture, this finding suggests that these structural modifications of the ancillary NHC ligand, possibly combined with the reported effects of aromaticity,[111] may affect the selectivity, allowing for new reaction pathways, in which, for instance, one can use highly aromatically stabilized substrates for selectively obtaining 5-*endo* products. Clearly, further work on these aspects is needed which may shed light on and rationalize the ligand effects on these peculiar reaction pathways in the intriguing framework of the dual-gold-catalysis.

Conclusions

In this work, we applied the Charge Displacement (and the Energy Decomposition) Analysis for investigating the Au-C bond in terms of the Dewar-Chatt-Duncanson coordination bond components in a series of 16 gold-acetylide complexes bearing different NHC ancillary ligands (NHC-Au(I)-CCH) with selectively modified structures.

As a result, we show that the upon structural modifications of the NHC, the features of the Au-C bond can be modulated, with the net electron ligand-to-metal charge transfer upon formation of the bond spanning a range of almost 0.1 e. In particular, the tunable bond component is the π communication between the alkynyl (π-donor) and the NHC (π-acceptor) ligand, with the structure of the NHC ligand influencing the extent of the π-donation.

We show, in agreement with previously reported results[37], that by adding oxygen atoms on the backbone of the NHC, thus increasing its capability of accepting π-electron charge via mesomeric effect, its π-acceptor properties are enhanced, with the charge transfer associated to the π-donation increasing over 0.1 e. We also show that we can efficiently tune the π-donation from the alkynyl in complexes bearing oxygen atoms by increasing the size of the ring of the NHC, by removing one oxygen and by using electron-donating groups on the nitrogen atoms. Finally, we demonstrate that the heteroatom substitution in the ring only slightly enhances the π-donation from the alkynyl.

We also address the potentialities of NMR spectroscopy in revealing the above discussed changes in the electronic structure of these complexes. Indeed, while both geometrical parameters and the alkynyl's C1-C2 stretching frequency have no significant correlation with the bonding parameters. the computed NMR nuclear shielding on the terminal carbon atom (C2) tightly correlates with the extent of the π-donation. This result can be rationalized on the basis of the electron charge deshielding on this atom by this tunable π communication bond component which adds on top of a significant polarization (charge shift from the C2 towards C1) of the alkynyl. This relationship can be extended to more realistic gold phenylethynyl complexes, thus making this model more general.

Finally, we made an attempt to isolate the effect of the Au-C bond tuning in the dual-gold-catalyzed Bergman cyclization. By using a more π-accepting NHC as ancillary ligand in the gold-alkynyl moiety of the reactant, we are able to modulate the activation barrier and the stability of the product. On the basis of the distortion/interaction analysis, we show that a

10.1002/ejic.202100260

higher barrier can be obtained because of a decreased ability of the more π-accepting NHC to stabilize the β-cation formed in the reaction. This finding may be of interest for modulating the selectivity of 5-*endo* versus 6-*endo* products in the framework of dual-gold-catalyzed cycloaromatizations.

By highlighting how the features of the Au-C bond can be significantly modified by selected structural modifications of the ancillary ligand and by providing evidence about their impact on their experimental characterization and reactivity, this study provides further insights for a rational design and analysis of gold-alkynyl complexes bearing ancillary NHC ligands with selected electronic properties.

References

[1] J. C. Lima, L. Rodríguez, *Chem. Soc. Rev.* **2011**, *40*, 5442–5456.

[2] A. De Nisi, C. Bergamini, M. Leonzio, G. Sartor, R. Fato, M. Naldi, M. Monari, N. Calonghi, M. Bandini, *Dalt. Trans.* **2016**, *45*, 1546–1553.

[3] E. Cerrada, V. Fernández-Moreira, M. C. Gimeno, in *Adv. Organomet. Chem.*, Academic Press Inc., **2019**, pp. 227–258.

[4] Z. Yang, G. Jiang, Z. Xu, S. Zhao, W. Liu, *Coord. Chem. Rev.* **2020**, *423*, 213492.

[5] M. Pujadas, L. Rodríguez, *Coord. Chem. Rev.* **2020**, *408*, 213179.

[6] V. W. W. Yam, K. M. C. Wong, *Top. Curr. Chem.* **2005**, *257*, 1–32.

[7] V. Gandon, *Angew. Chemie Int. Ed.* **2012**, *51*, 11200–11200.

[8] S. A. Shahzad, M. A. Sajid, Z. A. Khan, D. Canseco-Gonzalez, *Synth. Commun.* **2017**, *47*, 735–755.

[9] S. B. Alyabyev, I. P. Beletskaya, *Russ. Chem. Rev.* **2017**, *86*, 689–749.

[10] S. B. Alyabyev, I. P. Beletskaya, *Russ. Chem. Rev.* **2018**, *87*, 984–1047.

[11] A. S. K. Hashmi, *Acc. Chem. Res.* **2014**, *47*, 864–876.

[12] X. Zhao, M. Rudolph, A. S. K. Hashmi, *Chem. Commun.* **2019**, *55*, 12127–12135.

[13] C. J. V. Halliday, J. M. Lynam, *Dalt. Trans.* **2016**, *45*, 12611–12626.

[14] G. Dos Passos Gomes, I. V. Alabugin, *J. Am. Chem. Soc.* **2017**, *139*, 3406–3416.

[15] H. T. Liu, X. G. Xiong, P. Diem Dau, Y. L. Wang, D. L. Huang, J. Li, L. S. Wang, *Nat. Commun.* **2013**, *4*, 1-7.

[16] G. Zhang, H. Wang, H. Yue, H. Li, S. Zhang, L. Fu, *J. Mol. Model.* **2015**, *21*, 5–9.

[17] I. J. B. Lin, C. S. Vasam, *Can. J. Chem.* **2005**, *83*, 812–825.

[18] N. Marion, S. P. Nolan, *Chem. Soc. Rev.* **2008**, *37*, 1776–1782.

[19] D. Gatineau, J.-P. Goddard, V. Mouriès-Mansuy, L. Fensterbank, *Isr. J. Chem.* **2013**, *53*, 892–900.

[20] H. V. Huynh, *Chem. Rev.* **2018**, *118*, 9457–9492.

[21] K. V. S. Ranganath, S. Onitsuka, A. K. Kumar, J. Inanaga, *Catal. Sci. Technol.* **2013**, *3*, 2161–2181.

[22] A. J. Arduengo, R. L. Harlow, M. Kline, *J. Am. Chem. Soc.* **1991**, *113*, 361–363.

[23] V. Lavallo, Y. Canac, C. Präsang, B. Donnadieu, G. Bertrand, *Angew. Chemie Int. Ed.* **2005**, *44*, 5705–5709.

[24] M. Braun, W. Frank, G. J. Reiss, C. Ganter, *Organometallics* **2010**, *29*, 4418–4420.

[25] T. W. Hudnall, C. W. Bielawski, *J. Am. Chem. Soc.* **2009**, *131*, 16039–16041.

[26] V. César, N. Lugan, G. Lavigne, *Eur. J. Inorg. Chem.* **2010**, *2010*, 361–365.

[27] D. M. Andrada, N. Holzmann, T. Hamadi, G. Frenking, *Beilstein J. Org. Chem.* **2015**, *11*, 2727–2736.

[28] H. V. Huynh, G. Frison, *J. Org. Chem.* **2013**, *78*, 328–338.

[29] D. Munz, *Organometallics* **2018**, *37*, 275–289.

[30] A. Liske, K. Verlinden, H. Buhl, K. Schaper, C. Ganter, *Organometallics* **2013**, *32*, 5269–5272.

[31] K. Verlinden, H. Buhl, W. Frank, C. Ganter, *Eur. J. Inorg. Chem.* **2015**, *2015*, 2416–2425.

[32] O. Back, M. Henry-Ellinger, C. D. Martin, D. Martin, G. Bertrand, *Angew. Chemie - Int. Ed.* **2013**, *52*, 2939–2943.

[33] X. Hu, Y. Tang, P. Gantzel, K. Meyer, *Organometallics* **2003**, *22*, 612–614.

[34] H. Jacobsen, A. Correa, C. Costabile, L. Cavallo, *J. Organomet. Chem.* **2006**, *691*, 4350–4358.

[35] D. J. Nelson, S. P. Nolan, *Chem. Soc. Rev.* **2013**, *42*, 6723–6753.

[36] M. N. Hopkinson, C. Richter, M. Schedler, F. Glorius, *Nature* **2014**, *510*, 485–496.

[37] C. A. Gaggioli, G. Bistoni, G. Ciancaleoni, F. Tarantelli, L. Belpassi, P. Belanzoni, *Chem. - A Eur. J.* **2017**, *23*, 7558–7569.

[38] P. Zargaran, T. Wurm, D. Zahner, J. Schießl, M. Rudolph, F. Rominger, A. S. K. Hashmi, *Adv. Synth. Catal.* **2018**, *360*, 106–111.

[39] G. Bistoni, S. Rampino, F. Tarantelli, L. Belpassi, *J. Chem. Phys.* **2015**, *142*, 084112.

[40] J. Oberkofler, B. Aikman, R. Bonsignore, A. Pöthig, J. Platts, A. Casini, F. E. Kühn, *Eur. J. Inorg. Chem.* **2020**, *2020*, 1040–1051.

[41] L. Belpassi, I. Infante, F. Tarantelli, L. Visscher, *J. Am. Chem. Soc.* **2008**, *130*, 1048–1060.

[42] N. Salvi, L. Belpassi, F. Tarantelli, *Chem. - A Eur. J.* **2010**, *16*, 7231–7240.

[43] E. Ronca, L. Belpassi, F. Tarantelli, *ChemPhysChem* **2014**, *15*, 2682–2687.

[44] D. Cappelletti, A. Bartocci, F. Grandinetti, S. Falcinelli, L. Belpassi, F. Tarantelli, F. Pirani, *Chem. - A Eur. J.* **2015**, *21*, 6234–6240.

[45] A. Bartocci, L. Belpassi, D. Cappelletti, S. Falcinelli, F. Grandinetti, F. Tarantelli, F. Pirani, *J. Chem. Phys.* **2015**, *142*, 184304.

[46] G. Bistoni, L. Belpassi, F. Tarantelli, *Angew. Chemie - Int. Ed.* **2013**, *52*, 11599–11602.

[47] C. A. Gaggioli, G. Ciancaleoni, D. Zuccaccia, G. Bistoni, L. Belpassi, F. Tarantelli, P. Belanzoni, *Organometallics* **2016**, *35*, 2275-2285.

[48] D. Zuccaccia, L. Belpassi, L. Rocchigiani, F. Tarantelli, A. Macchioni, *Inorg. Chem.* **2010**, *49*, 3080–3082.

[49] F. Pirani, D. Cappelletti, S. Falcinelli, D. Cesario, F. Nunzi, L. Belpassi, F. Tarantelli, *Angew. Chemie - Int. Ed.* **2019**, *58*, 4195–4199.

[50] M. Mitoraj, A. Michalak, *J. Mol. Model.* **2007**, *13*, 347–355.

[51] A. Michalak, M. Mitoraj, T. Ziegler, *J. Phys. Chem. A* **2008**, *112*, 1933–1939.

[52] R. F. Nalewajski, J. ozek, *Int. J. Quantum Chem.* **1994**, *51*, 187–200.

[53] R. F. Nalewajski, J. Mrozek, A. Michalak, *Int. J. Quantum Chem.* **1997**, *61*, 589–601.

[54] T. Lu, F. Chen, *J. Phys. Chem. A* **2013**, *117*, 3100–3108.

[55] F. Nunzi, D. Cesario, F. Pirani, L. Belpassi, G. Frenking, F. Grandinetti, F. Tarantelli, *J. Phys. Chem. Lett.* **2017**, *8*, 3334–3340.

[56] D. Sorbelli, L. Belpassi, F. Tarantelli, P. Belanzoni, *Inorg. Chem.* **2018**, *57*, 6161-6175.

[57] L. Gregori, D. Sorbelli, L. Belpassi, F. Tarantelli, P. Belanzoni, *Inorg. Chem.* **2019**, *58*, 3115-3129.

[58] D. Sorbelli, L. Nunes dos Santos Comprido, G. Knizia, A. S. K. Hashmi, L. Belpassi, P. Belanzoni, J. E. M. N. Klein, *ChemPhysChem* **2019**, *20*, 1671–1679.

[59] G. Ciancaleoni, L. Biasiolo, G. Bistoni, A. Macchioni, F. Tarantelli, D. Zuccaccia, L. Belpassi, *Chem. - A Eur. J.* **2015**, *21*, 2467–2473.

[60] G. Bistoni, S. Rampino, N. Scafuri, G. Ciancaleoni, D. Zuccaccia, L. Belpassi, F. Tarantelli, *Chem. Sci.* **2016**, *7*, 1174–1184.

[61] D. Marchione, M. A. Izquierdo, G. Bistoni, R. W. A. Havenith, A. Macchioni, D. Zuccaccia, F. Tarantelli, L. Belpassi, *Chem. - A Eur. J.* **2017**, *23*, 2722–2728.

[62] M. A. Izquierdo, F. Tarantelli, R. Broer, G. Bistoni, L. Belpassi, R. W. A. Havenith, *Eur. J. Inorg. Chem.* **2020**, *2020*, 1177–1183.

[63] M. De Santis, S. Rampino, H. M. Quiney, L. Belpassi, L. Storchi, *J. Chem. Theory Comput.* **2018**, *14*, 1286–1296.

[64] M. De Santis, S. Rampino, L. Storchi, L. Belpassi, F. Tarantelli, *Inorg. Chem.* **2019**, *58*, 11716–11729.

[65] E. Rossi, M. De Santis, D. Sorbelli, L. Storchi, L. Belpassi, P. Belanzoni, *Phys. Chem. Chem. Phys.* **2020**, *22*, 1897–1910.

[66] D. Sorbelli, M. De Santis, P. Belanzoni, L. Belpassi, *J. Phys. Chem. A* **2020**, *124*, 10565–10579.

[67] F. M. Bickelhaupt, E. J. Baerends, in *Rev. Comput. Chem.*, Wiley-VCH Verlag, **2007**, pp. 1–86.

[68] M. P. Mitoraj, A. Michalak, T. Ziegler, *J. Chem. Theory Comput.* **2009**, *5*, 962–975.

[69] *ADF Manual ADF Program System Release 2014*, **1993**.

[70] G. te Velde, F. M. Bickelhaupt, E. J. Baerends, C. Fonseca Guerra, S. J. A. van Gisbergen, J. G. Snijders, T. Ziegler, *J. Comput. Chem.* **2001**, *22*, 931–967.

[71] A. D. Becke, *Phys. Rev. A* **1988**, *38*, 3098–3100.

[72] J. P. Perdew, *Phys. Rev. B* **1986**, *33*, 8822–8824.

[73] E. Van Lenthe, E. J. Baerends, J. G. Snijders, *J. Chem. Phys.* **1993**, *99*, 4597–4610.

[74] E. Van Lenthe, E. J. Baerends, J. G. Snijders, *J. Chem. Phys.* **1994**, *101*, 9783–9792.

[75] E. Van Lenthe, *J. Chem. Phys.* **1999**, *110*, 8943–8953.

[76] S. Grimme, J. Antony, S. Ehrlich, H. Krieg, *J. Chem. Phys.* **2010**, *132*, 154104.

[77] S. Grimme, S. Ehrlich, L. Goerigk, *J. Comput. Chem.* **2011**, *32*, 1456–1465.

[78] "GitHub - BERTHA-4c-DKS/pycubescd," can be found under https://github.com/BERTHA-4c-DKS/pycubescd

[79] P. J. Stephens, F. J. Devlin, C. F. Chabalowski, M. J. Frisch, *J. Phys. Chem.* **1994**, *98*, 11623–11627.

[80] L. Rocchigiani, J. Fernandez-Cestau, I. Chambrier, P. Hrobárik, M. Bochmann, *J. Am. Chem. Soc.* **2018**, *140*, 8287–8302.

[81] A. H. Greif, P. Hrobárik, M. Kaupp, *Chem. - A Eur. J.* **2017**, *23*, 9790–9803.

[82] M. Ernzerhof, G. E. Scuseria, *J. Chem. Phys.* **1999**, *110*, 5029–5036.

[83] C. Adamo, V. Barone, *J. Chem. Phys.* **1999**, *110*, 6158–6170.

[84] A. E. Hansen, T. D. Bouman, *J. Chem. Phys.* **1985**, *82*, 5035–5047.

[85] J. Autschbach, *Mol. Phys.* **2013**, *111*, 2544–2554.

[86] M. Swart, F. M. Bickelhaupt, *J. Comput. Chem.* **2008**, *29*, 724–734.

[87] G. Ciancaleoni, S. Rampino, D. Zuccaccia, F. Tarantelli, P. Belanzoni, L. Belpassi, *J. Chem. Theory Comput.* **2014**, *10*, 1021–1034.

[88] C. Fonseca Guerra, J.-W. Handgraaf, E. J. Baerends, F. M. Bickelhaupt, *J. Comput. Chem.* **2004**, *25*, 189–210.

[89] C. C. Pye, T. Ziegler, *Theor. Chem. Acc.* **1999**, *101*, 396–408.

[90] C. Riplinger, B. Sandhoefer, A. Hansen, F. Neese, *J. Chem. Phys.* **2013**, *139*, 134101.

[91] C. Riplinger, F. Neese, *J. Chem. Phys.* **2013**, *138*, 34106.

[92] F. Neese, *Wiley Interdiscip. Rev. Comput. Mol. Sci.* **2012**, *2*, 73–78.

[93] C. Riplinger, P. Pinski, U. Becker, E. F. Valeev, F. Neese, *J. Chem. Phys.* **2016**, *144*, 24109.

[94] D. G. Liakos, F. Neese, *J. Chem. Theory Comput.* **2015**, *11*, 4054–4063.

[95] D. Andrae, U. Häußermann, M. Dolg, H. Stoll, H. Preuß, *Theor. Chim. Acta* **1990**, *77*, 123–141.

[96] D. G. Liakos, M. Sparta, M. K. Kesharwani, J. M. L. Martin, F. Neese, *J. Chem. Theory Comput.* **2015**, *11*, 1525–1539.

[97] I. Ferná, F. M. Bickelhaupt, *Chem. Soc. Rev* **2014**, *43*, 4953.

[98] F. M. Bickelhaupt, K. N. Houk, *Angew. Chemie - Int. Ed.* **2017**, *56*, 10070–10086.

[99] P. Vermeeren, S. C. C. van der Lubbe, C. Fonseca Guerra, F. M. Bickelhaupt, T. A. Hamlin, *Nat. Protoc.* **2020**, *15*, 649–667.

[100] L. Biasiolo, L. Belpassi, C. A. Gaggioli, A. Macchioni, F. Tarantelli, G. Ciancaleoni, D. Zuccaccia, *Organometallics* **2016**, *35*, 595–604.

[101] C. Poggel, G. Frenking, *Chem. – A Eur. J.* **2018**, *24*, 11675–11682.

[102] C. A. Gaggioli, L. Belpassi, F. Tarantelli, P. Belanzoni, *Chem. Commun.* **2017**, *53*, 1603–1606.

[103] S. V. C. Vummaleti, D. J. Nelson, A. Poater, A. Gómez-Suárez, D. B. Cordes, A. M. Z. Slawin, S. P. Nolan, L. Cavallo, *Chem. Sci.* **2015**, *6*, 1895–1904.

[104] R. K. Mohamed, P. W. Peterson, I. V. Alabugin, *Chem. Rev.* **2013**, *113*, 7089–7129.

[105] B. Gold, N. E. Shevchenko, N. Bonus, G. B. Dudley, I. V. Alabugin, *J. Org. Chem.* **2012**, *77*, 75–89.

[106] B. Gold, G. B. Dudley, I. V. Alabugin, *J. Am. Chem. Soc.* **2013**, *135*, 1558–1569.

[107] B. Gold, P. Batsomboon, G. B. Dudley, I. V. Alabugin, *J. Org. Chem.* **2014**, *79*, 6221–6232.

[108] M. R. Aronoff, B. Gold, R. T. Raines, *Org. Lett.* **2016**, *18*, 1538–1541.

[109] M. M. Hansmann, M. Rudolph, F. Rominger, A. S. K. Hashmi, *Angew. Chemie Int. Ed.* **2013**, *52*, 2593–2598.

[110] L. Ye, Y. Wang, D. H. Aue, L. Zhang, *J. Am. Chem.Soc* **2012**, *134*, 8.

[111] M. M. Hansmann, S. Tšupova, M. Rudolph, F. Rominger, A. S. K. Hashmi, *Chem. - A Eur. J.* **2014**, *20*, 2215–2223.

10.1002/ejic.202100260

Entry for Table of Contents

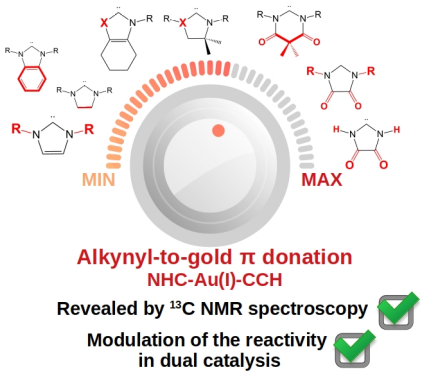

Tuning of the gold(I)-carbon bond features in gold-alkynyl complexes can be I) accomplished by structural modifications of the NHC ancillary ligand; ii) revealed through NMR spectroscopy; and iii) could affect the reactivity in dual-gold catalysis.